http://dx.doi.org/10.6113/TKPE.2016.21.2.134

토크 리플 저감을 위한 새로운 비대칭 하프-타입 영구자석 매입형 브러시리스 직류 모터 구조

심요섭[1], 니구치 노보루[1], 히라타 카츠히로†

A Novel Asymmetrical Half-type IPM BLDC Motor Structure for Reducing Torque Ripple

Yosub Sim[1], Noboru Niguchi[1], and Katsuhiro Hirata†

Abstract

This paper proposes a novel asymmetrical interior permanent magnet (IPM) brushless DC (BLDC) motor structure, which utilizes half-type permanent magnet (PM) configuration and has asymmetrical side gaps (slot next to the PMs) for reducing torque ripples. This structure uses 24% less volume of PMs than conventional IPM BLDC motor with a full set of magnets. The characteristics of the proposed motor are compared with three other half-type IPM BLDC motors through finite elements method (FEM) analysis, and the usefulness of the proposed motor was verified through experimental evaluation on prototypes of the conventional motor and proposed motor under various torque load conditions. This research obtained a high-performance IPM BLDC motor while decreasing manufacturing cost at the same time.

Key words: Air gaps, Brushless motors, Finite element analysis, Permanent magnets

1. Introduction

High performance BLDC motors with low manufacturing cost are very important in many industries. Research on torque ripple reduction of motors is especially an important issue since it is related to the vibration, noise and efficiency of the motor, and these elements directly affect the fuel consumption of the motors.

In general, BLDC motors comprises of a shaft, rotor, PM, stator and coils. The characteristics of the motor are considerably influenced by the design of these elements. Because of this, many laboratories and companies conduct research on novel motor structures that can achieve high performance while also maintaining low manufacturing cost.

[1] proposed mathematical frequency equations of back Electromotive Force (EMF), cogging torque and Unbalanced Magnetic Force (UMF) of a BLDC motor. They forecasted that using the proposed equations, vibration and noise which are caused by uneven magnetization of PMs can be reduced. [2] managed to increase the back EMF and at the same time decrease the cogging torque and Total Harmonic Distortion (THD) by using anisotropic ferrite magnets and optimizing the magnetizing direction of the magnets. In [3], they optimized the shape of the PMs in a Surface Mounted Permanent Magnet (SPM) BLDC motor. They were able to obtain sinusoidal shaped back EMF waveforms and reduced torque ripples without significant reduction in efficiency. [4] investigated the influence of electric loading conditions and step-skewed rotors on cogging torque, back EMF and torque ripples of PM machines. They concluded that the actual cogging torque and electromagnetic

Paper number: TKPE-2016-21-2-6
Print ISSN: 1229-2214 Online ISSN: 2288-6281
† Corresponding author: k-hirata@ams.eng.osaka-u.ac.jp, Dept. of Adaptive Machine Systems, Graduate School of Engineering, Osaka University
Tel: +81-6-6879-7533 Fax: +81-6-6879-7533
[1] Dept. of Adaptive Machine Systems, Graduate School of Engineering, Osaka University
Manuscript received Aug. 10, 2015; revised Sep. 16, 2015; accepted Nov. 18, 2015

torque ripple can be reduced by one actual cogging period skew. In addition,[5],[6] also proposed novel motor structures for obtaining high performance motors by reducing torque ripples.

In this research, a novel asymmetrical half-type IPM BLDC motor is proposed. The PM volume used has been reduced by 24 % compared to conventional IPM BLDC motor. However, initial analyses showed that the torque ripple increased. This problem was tackled by adjusting the side gaps (slot next to the PMs) and making them asymmetrical. Although some studies such as[7]-[9] have researched on the half-type PM motors, they did not consider how to reduce the torque ripple of them by side gaps. Also, many industries carefully have considered to apply half-type IPM BLDC motors to their actual physical actuator systems since they could not make a novel idea for reducing torque ripples of them. Because of this reason, this research focuses on torque ripple reduction of half-type IPM BLDC motors by considering side gaps under square drive signal.

First, the characteristics of the asymmetrical half-type IPM BLDC motor were determined by FEM analysis. Then, a prototype was manufactured and the experimental evaluation results were compared with those of the FEM analyses. We expect this high performance IPM BLDC motor with reduced manufacturing cost to be implemented in many fields [10].

2. Design of the proposed asymmetrical half-type IPM BLDC motor

In this research, both of conventional IPM BLDC motor and the proposed asymmetrical half-type IPM BLDC motor were designed according to the target motor specification. Table I shows the target motor specification.

Fig 1 shows a conventional IPM BLDC motor that we designed and close up illustration of the side gaps. In the conventional IPM BLDC motor, parallel magnetized PMs are inserted inside the rotor, with neighboring magnets magnetized in opposite directions of each other. On the other hand, Fig 2 shows the proposed asymmetrical half-type IPM BLDC motor and close up illustration of the side gaps. Only half the number of PMs has been used, with all the magnets magnetized in the same direction. Also, the side gaps of the magnetless side have been widened, and the side gaps are asymmetrical. The rotors of both motors are flower-shaped for generating trapezoidal-shaped EMF signals as well as decreasing cogging torque. Since the EMF and motor drive signals are similar in shape, torque ripples will be decreased. In addition, the magnetization pattern of the PMs in both IPM BLDC motors is parallel since the shape of the PMs is cuboid.

TABLE I
TARGET MOTOR SPECIFICATION

Parameter	Value [Unit]
Input voltage	13.5 [V]
Drive signal type	Square waveform
Max. drive temperature	150 [℃]
Torque range	0.5 ~ 1.5 [Nm]
Min. rotation speed	2100 [rpm] (at 1.5 Nm)
Max. phase current	35 [Arms] (at 1.5 Nm)
Efficiency	Over 80 [%] (at every torque load)

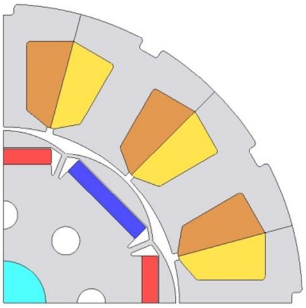
(a) 2D model

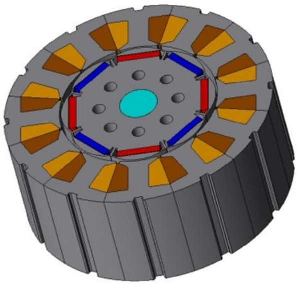
(b) 3D model

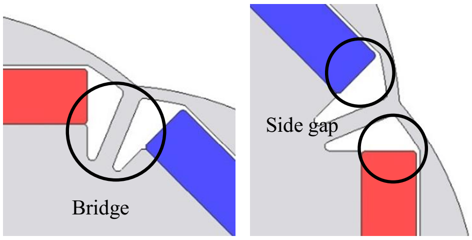

(c) Side gaps (slot next to the PMs)

Fig. 1. Conventional IPM BLDC motor.

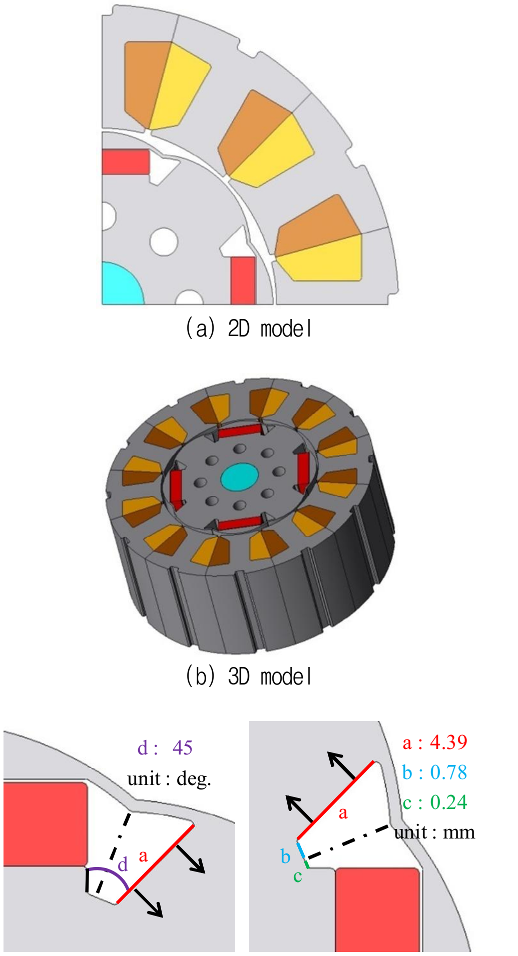

(a) 2D model

(b) 3D model

(c) Asymmetrical side gaps (slot next to the PMs)

Fig. 2. Asymmetrical half-type IPM BLDC motor.

To design the asymmetrical side gaps in the half-type IPM BLDC motor, the thin bridges were removed and lines "a" were offset to the direction of an arrow by maintaining angle (see Fig 2(c)). As offsetting lines "a", the side gaps of the magnetless side were widened than those of the magnet inserted side. The dotted lines of Fig 2(c) are center lines of the symmetrical side gaps.

In the cases of the same type side gaps to those of the conventional IPM BLDC motor or symmetrical side gaps without the thin bridges, flows of magnetic flux which pass the parts those having magnets (magnet inserted side) and those do not having magnets (magnetless side) can be affected differently since materials of the both parts are different each other. Also, the magnetic flux density distribution in the air gap of magnet inserted side and magnetless side can be asymmetrical-shaped, and this causes the large torque ripples. Because of these reasons, it is expected that the torque ripple can be reduced by designing the side gaps asymmetrically. The FEM analysis of the magnetic flux density distribution in the air gap is implemented in section 3.

Also, there are two important advantages to the proposed asymmetrical half-type IPM BLDC motor. First, it is possible to decrease the number and volume of PMs for obtaining almost the same characteristics with that of the conventional IPM BLDC motor since the leakage flux is decreased, and this makes it possible to make almost the same torque constant with that of the conventional IPM BLDC motor. Because of this reason, it is also possible to decrease manufacturing cost.

Second, it is advantageous to decrease motor size. As shown in Figs 1 and 2, the proposed asymmetrical half-type IPM BLDC motor uses thicker PMs than those of the conventional IPM BLDC motor. In this case, it is possible to use the PMs which have the high residual magnetic flux, high grade PMs, to the proposed asymmetrical half-type IPM BLDC motor without demagnetization of the PMs since the magnet thickness, which composes the leakage flux loop, is thick, and this makes the working point of the PMs high. However, it is impossible to use the PMs which have the high residual magnetic flux, high grade PMs, to the conventional IPM BLDC motor since the magnet thickness, which composes the leakage flux loop, is thin, and this makes the working point of the PMs low with high possibility of demagnetization of the PMs. Because of this reason, downsizing the proposed asymmetrical half-type IPM BLDC motor is more advantageous than that of the conventional IPM BLDC motor using the high grade PMs.

3. FEM analysis

In this research, analyses were carried out by coupling the FEM models of the 8 pole 12 slot BLDC motor with a 3 phase switching electrical circuit. The 3 phase switching electrical circuit outputs U, V, W 6 step square waveform drive signals according to the rotation angle. Fig 3 shows the schematic diagram of the 3 phase switching electrical circuit with FEM BLDC motor coils.

In this section, the two IPM BLDC motors in the previous section are also compared with three other half-type IPM BLDC motors to verify the usefulness of the proposed asymmetrical half-type IPM BLDC

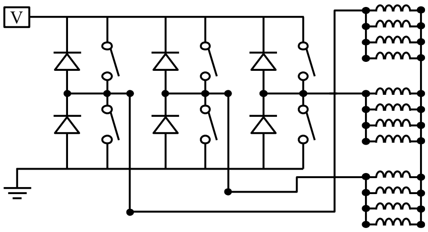

Fig. 3. 3 phase switching electrical circuit.

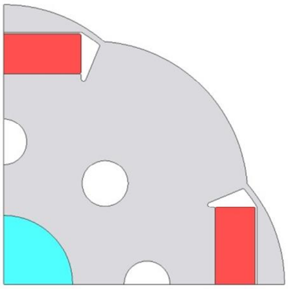

(a) Rotor structure

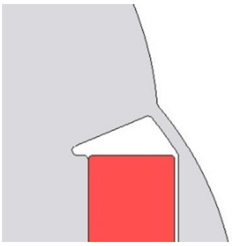

(b) Side gap

Fig. 4. Characteristics of model 1.

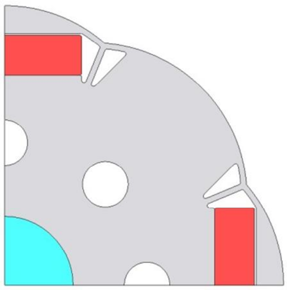

(a) Rotor structure

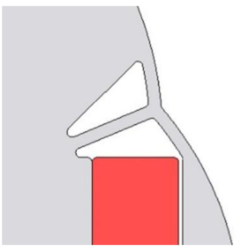

(b) Side gap

Fig. 5. Characteristics of model 2.

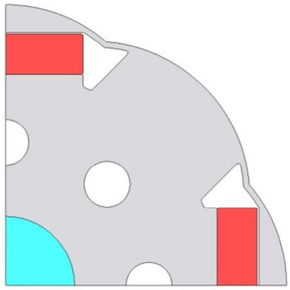

(a) Rotor structure

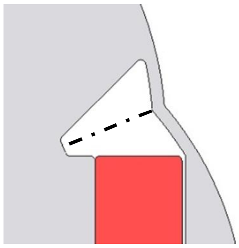

(b) Side gap

Fig. 6. Characteristics of model 3.

motor. Figs 4, 5 and 6 show the rotor structures of the other three half-type IPM BLDC motors and close up illustrations of the side gaps.

Models 1, 2 and 3 are similar to the conventional IPM BLDC motor. However, the PMs in which S poles face stator have been removed, and everything in that pole including side gaps has been filled in with electrical steel in Model 1 (see Fig 4). On the other hand, the side gaps which locate at the parts those do not having magnets were maintained with the thin bridges in Model 2 (see Fig 5). The side gaps of Model 2 are the same type to those of the conventional IPM BLDC motor. And the side gaps which locate at the parts those having magnets and those do not having magnets were combined symmetrically by removing the thin bridges in Model 3 (see Fig 6).

The difference between the proposed asymmetrical half-type IPM BLDC motor and Model 3 is the shape of side gaps. In the case of the proposed asymmetrical half-type IPM BLDC motor, the side gaps which locate at the parts those do not having magnets are widened, and the area of them is bigger than that of the side gaps which locate at the parts those having magnets (see Fig 2(c)). Because of this reason, it is expected to obtain more symmetrical-shaped magnetic flux density distribution in the air gap of magnet inserted side and magnetless side. However, the area of the side gaps which locate

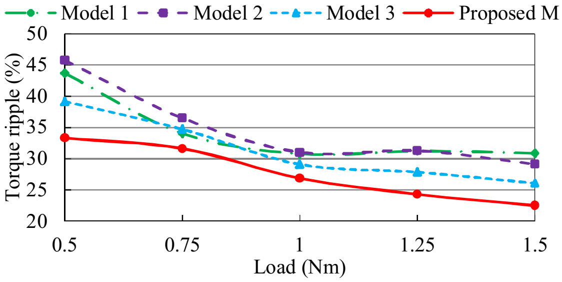

Fig. 7. Torque ripples of half-type IPM BLDC motors.

at the parts those having magnets and those do not having magnets of Model 3 are the same since they were combined symmetrically (see Fig 6). In this case, the magnetic flux density distribution in the air gap of magnet inserted side and magnetless side becomes less symmetrical-shaped since materials of magnet inserted side and magnetless side are different each other.

First, to determine the torque ripple characteristics of all the half-type IPM BLDC motors, FEM analysis was carried out under various torque load conditions. In this analysis, the characteristics during steady state operation were analyzed. Fig 7 shows the torque ripples of each half-type IPM BLDC motor and Table II summarizes the analysis results. Since EMF and phase current waveforms are not trapezoidal-shaped at high rotation speeds under square drive signal with torque load conditions, it is not easy to estimate the torque ripple from the EMF waveform. However, through FEM analysis, the torque ripple of each half-type IPM BLDC motor could be determined. As shown in Fig 7 and Table II, the torque ripple of the proposed asymmetrical half-type IPM BLDC motor shows a lower tendency than those of three other half-type IPM BLDC motors at every torque load condition. This means that the vibration and noise of the half-type IPM BLDC motor can be reduced effectively by applying the asymmetrical side gaps.

The reason why the torque ripple of the proposed asymmetrical half-type IPM BLDC motor shows a lower tendency than those of three other half-type IPM BLDC motors, is that the magnetic flux density distribution in the air gap of magnet inserted side (PM side) and magnetless side (Non-PM side) of the proposed asymmetrical half-type IPM BLDC motor are more symmetrical-shaped compared to those of three other half-type IPM BLDC motors. Fig 8 shows the magnetic flux density in the air gap of all the half-type IPM BLDC motors with input switching

TABLE II
TORQUE RIPPLE ANALYSIS RESULTS
(HALF-TYPE IPM BLDC MOTORS)

Load [Nm]	Torque ripple [%]			
	Model 1	Model 2	Model 3	Proposed model
0.50	43.68	45.78	39.17	33.33
0.75	34.06	36.50	34.73	31.63
1.00	30.78	31.03	29.09	26.88
1.25	31.23	31.29	27.86	24.31
1.50	30.89	29.12	26.07	22.52

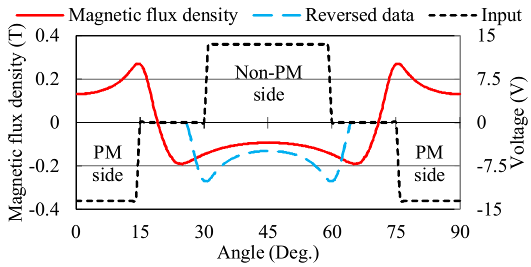

(a) Model 1

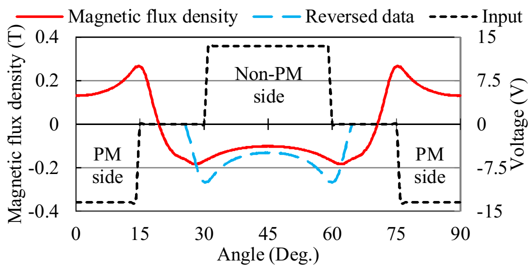

(c) Model 2

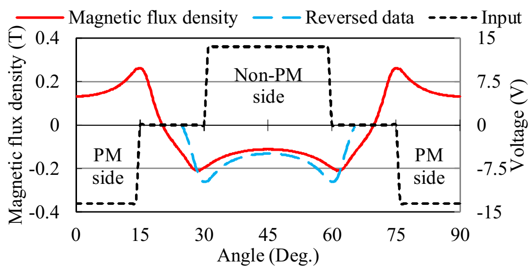

(c) Model 3

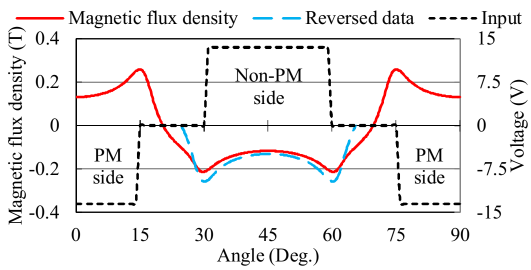

(d) Proposed model

Fig. 8. Magnetic flux density distribution in the air gap.

voltage which is described by using the mechanical angle.

TABLE III
MAGNETIC FLUX DENSITY DISTRIBUTION
IN THE AIR GAP ANALYSIS RESULTS

Angle [Deg.]	A difference of the magnetic flux density in the air gap between A and B [T]			
	Model 1	Model 2	Model 3	Proposed model
30	0.124	0.097	0.066	0.046
35	0.071	0.056	0.038	0.026
45	0.038	0.030	0.020	0.014
55	0.069	0.054	0.036	0.024
60	0.125	0.098	0.066	0.045
A : Magnet inserted side / B : Magnetless side				

When the magnetic flux creates the torque, the magnet inserted side and magnetless side are used. Because of this reason, the magnetic flux density distribution in the air gap of both sides should be symmetrical-shaped for reducing torque ripples. For comparing the magnetic flux density distribution in the air gap of both sides, the line, which shows the magnetic flux density distribution in the air gap of magnet inserted side, was reversed to the magnetless side (see reversed data line of Fig 8). In other words, the reversed data line and magnetic flux density line from 30 degree to 60 degree of Fig 8 show the magnetic flux density distribution in the air gap of magnet inserted side and magnetless side. Table III summarizes the analysis results.

As shown in the analysis results, a difference of the magnetic flux density in the air gap between magnet inserted side and magnetless side of the proposed asymmetrical half-type IPM BLDC motor shows a lower tendency than those of three other half-type IPM BLDC motors. Because of this reason, the magnetic flux density distribution in the air gap of magnet inserted side and magnetless side of the proposed asymmetrical half-type IPM BLDC motor became more symmetrical-shaped than those of three other half-type IPM BLDC motors, and this made a lower tendency of torque ripples.

Next, the conventional IPM BLDC motor and the proposed asymmetrical half-type IPM BLDC motor were compared using FEM analysis under various torque load conditions to verify the usefulness of the proposed asymmetrical half-type IPM BLDC motor. In this analysis, the various characteristics during steady state operation were analyzed.

Fig 9 shows the magnetic flux analysis result of the proposed asymmetrical half-type IPM BLDC motor. In the proposed asymmetrical half-type IPM BLDC motor, although the magnetic flux lines from one magnet does not enter into a neighboring magnet, a constant magnetic flux can be seen in the rotor and stator.

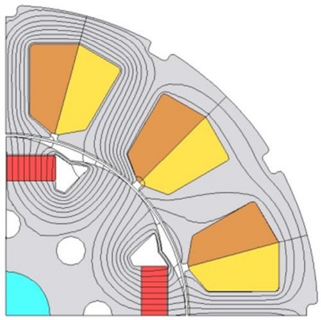

Fig. 9. Magnetic flux test result (Proposed model).

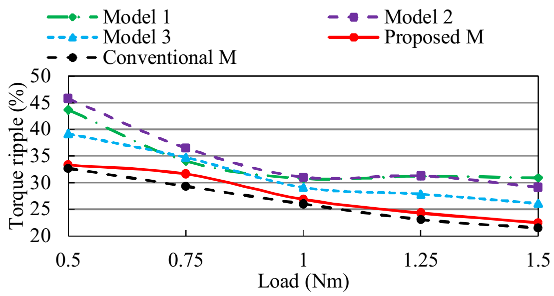

Fig. 10. Torque ripple test results (FEM analysis).

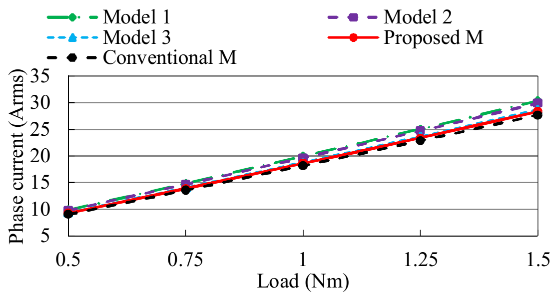

Fig. 11. Phase current test results (FEM analysis).

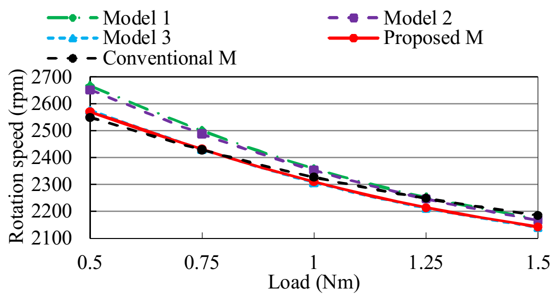

Fig. 12. Rotation speed test results (FEM analysis).

Figs 10, 11, 12 and 13 show the torque ripple,

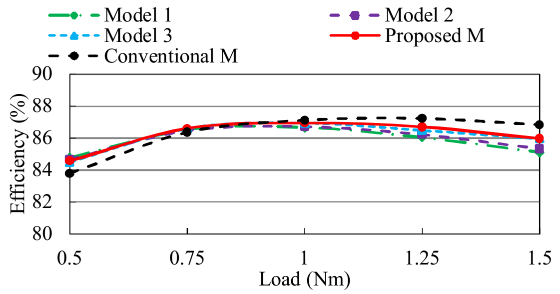

Fig. 13. Efficiency test results (FEM analysis).

TABLE IV
FEM ANALYSIS RESULTS

Contents	Load [Nm]	A	B	C	D	E
Torque ripple [%]	0.50	43.68	45.78	39.17	33.33	32.67
	0.75	34.06	36.50	34.73	31.63	29.35
	1.00	30.78	31.03	29.09	26.88	26.00
	1.25	31.23	31.29	27.86	24.31	23.07
	1.50	30.89	29.12	26.07	22.52	21.52
Phase current [Arms]	0.50	9.84	9.77	9.30	9.22	8.99
	0.75	14.81	14.67	14.00	13.86	13.54
	1.00	19.93	19.65	18.77	18.58	18.15
	1.25	25.06	24.73	23.62	23.38	22.86
	1.50	30.41	29.92	28.67	28.37	27.71
Rotation speed [rpm]	0.50	2667	2652	2576	2570	2549
	0.75	2500	2488	2431	2431	2429
	1.00	2359	2353	2308	2310	2327
	1.25	2252	2246	2212	2214	2248
	1.50	2172	2167	2140	2142	2185
Efficiency [%]	0.50	84.78	84.69	84.51	84.58	83.79
	0.75	86.54	86.48	86.61	86.62	86.38
	1.00	86.68	86.73	86.95	86.96	87.13
	1.25	86.05	86.23	86.49	86.71	87.24
	1.50	85.12	85.34	85.97	85.98	86.84
PMs amount [g]		50.3	50.3	50.3	50.3	66.1

A : Model 1 / B : Model 2 / C : Model 3
D : Proposed model / E : Conventional model

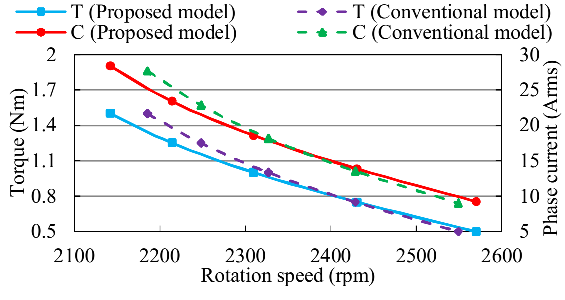

Fig. 14. N-T & N-I characteristics (FEM analysis).

phase current, rotation speed and efficiency FEM analysis results under various torque load conditions with those of Models 1, 2 and 3, and summarized FEM analysis results are presented in Table IV. In addition, Fig 14 shows the N-T and N-I characteristics of the conventional IPM BLDC motor and proposed asymmetrical half-type IPM BLDC motor.

As shown in the FEM analysis results, it was possible to reduce torque ripples effectively through the proposed asymmetrical half-type IPM BLDC motor, and this makes us to expect to decrease the noise and vibration using this IPM BLDC motor.

In addition, PM volume usage of the proposed asymmetrical half-type IPM BLDC motor was reduced 24 % than that of the conventional IPM BLDC motor to create almost the same characteristics with that of the conventional IPM BLDC motor. In the case of the proposed asymmetrical half-type IPM BLDC motor, side gaps which locate at the parts those having magnets and those do not having magnets are combined asymmetrically by removing the thin bridges, and this makes less magnetic flux leakage than that of the conventional IPM BLDC motor which has separated, T-shaped, side gaps by the thin bridges. Consequently, there exists enough magnetic flux in the rotor of the proposed asymmetrical half-type IPM BLDC motor for creating almost the same torque constant with that of the conventional IPM BLDC motor, and this obviates a need to increase motor size in spite of less PM volume usage under the same requirements of motor characteristics.

Also, from the N-T and N-I characteristics, it was proven that the proposed asymmetrical half-type IPM BLDC motor can be used under various torque load conditions without any problem like conventional IPM BLDC motor.

4. Experimental evaluation

Experimental evaluation was also carried out under various torque load conditions with prototypes of the conventional IPM BLDC motor and proposed asymmetrical half-type IPM BLDC motor to verify the FEM analysis results and usefulness of the proposed asymmetrical half-type IPM BLDC motor. Figs 15 and 16 show the rotor structures and assembled same-sized prototypes, and Fig 17 shows the experimental evaluation setup.

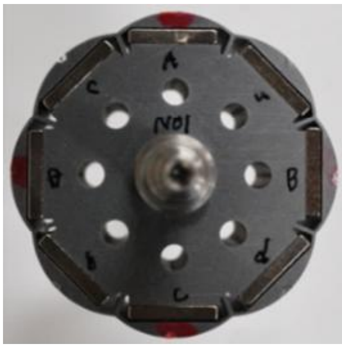

(a) Rotor structure

(b) Assembled prototype

Fig. 15. Conventional IPM BLDC prototype.

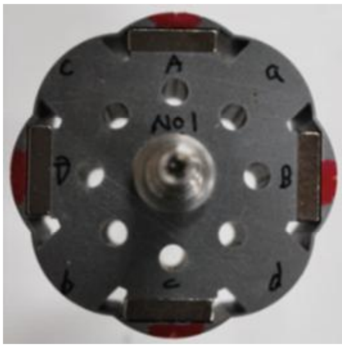

(a) Rotor structure

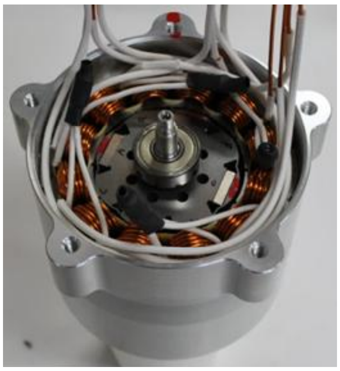

(b) Assembled prototype

Fig. 16. Asymmetrical half-type IPM BLDC prototype.

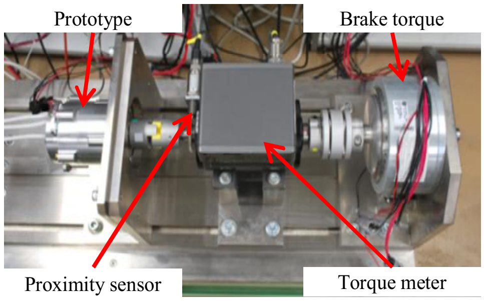

Fig. 17. Experimental evaluation setup.

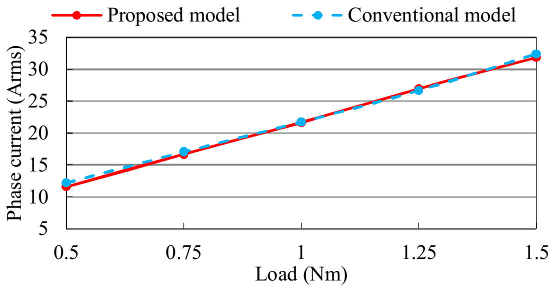

Fig. 18. Phase current test results (Experiments).

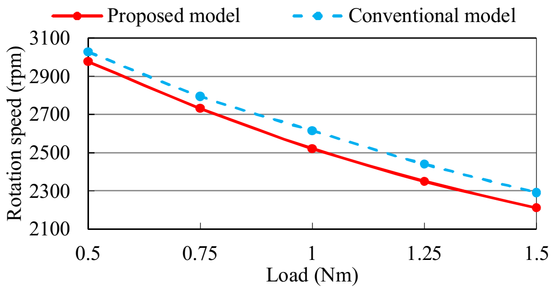

Fig. 19. Rotation speed test results (Experiments).

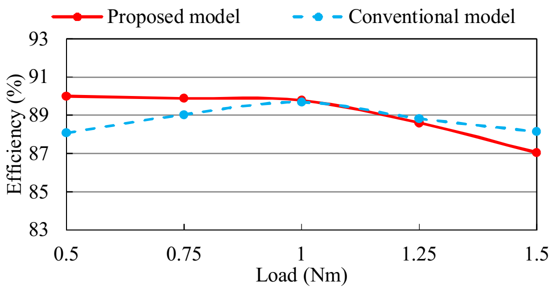

Fig. 20. Efficiency test results (Experiments).

Figs 18, 19 and 20 show the phase current, rotation speed and efficiency experimental evaluation results under various torque load conditions, and summarized experimental evaluation results are presented in Table V. In addition, Fig 21 shows the N-T and N-I characteristics of both prototypes.

TABLE V
EXPERIMENTAL EVALUATION RESULTS

Contents	Load [Nm]	Proposed model	Conventional model
Phase current [Arms]	0.50	11.58	12.17
	0.75	16.67	17.05
	1.00	21.66	21.72
	1.25	26.95	26.66
	1.50	31.86	32.42
Rotation speed [rpm]	0.50	2978	3028
	0.75	2733	2795
	1.00	2522	2616
	1.25	2351	2440
	1.50	2212	2292
Efficiency [%]	0.50	90.00	88.08
	0.75	89.89	89.04
	1.00	89.78	89.69
	1.25	88.61	88.83
	1.50	87.05	88.14

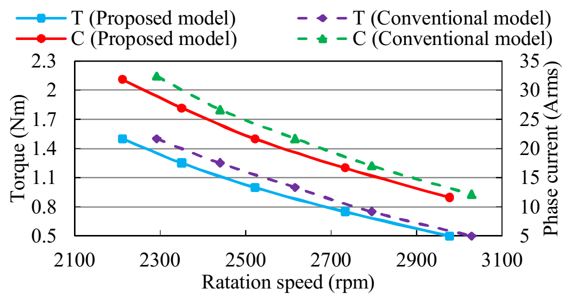

Fig. 21. N-T & N-I characteristics (Experiments).

As shown in Fig 19, torque of the proposed asymmetrical half-type IPM BLDC motor is lower only 0.10 Nm than that of the conventional IPM BLDC motor at 2300 rpm, and this difference decreases as increasing rotation speed. For example, torque differences of the both IPM BLDC motors are only 0.09 Nm and 0.06 Nm at 2500 rpm and 3000 rpm, respectively. These are insignificant differences that do not visibly affect the motor characteristics, and can be ignored.

Also, experimental evaluation results show that the phase current and rotation speed of the experimental evaluation are higher than those of the FEM analysis. The reason for this is that the bearing, which is located at the shaft, accidently became magnetized by the magnetic leakage of the PMs to the axial direction of the prototypes. Because of this reason, the torque constant of the prototypes decreased than those of the FEM BLDC motor models. Especially, the effect of the magnetic leakage of the PMs to the axial direction of the conventional IPM BLD motor was higher than that of the proposed asymmetrical half-type IPM BLDC motor since the PM volume usage was increased by 24 %, and this caused the phase current of the conventional IPM BLDC motor increased more than that of the proposed asymmetrical half-type IPM BLDC motor. In the next research step, this problem can be avoided by considering the magnetic leakage of the PMs to the axial direction of the motor structure through 3D FEM analysis and optimizing the motor structure with ensuring that there is enough space between the PMs and the bearing.

Although a difference between the FEM analysis and experimental evaluation results can be seen, Table V shows that the target motor specification has been satisfied in the experimental evaluation. Especially, it was possible to obtain the high efficiency by the proposed asymmetrical half-type IPM BLDC motor while decreasing manufacturing cost at the same time. Also, from the N-T and N-I characteristics, it was again proven that the proposed asymmetrical half-type IPM BLDC motor can be used under various torque load conditions by maintaining almost the same torque constant with those of the conventional IPM BLDC motor.

5. Conclusion

In this research, a novel asymmetrical half-type IPM BLDC motor was proposed. Its characteristics were calculated through FEM analysis and also determined through experimental evaluation on a prototype under various torque load conditions. The PM volume usage was reduced by 24 % than that of the conventional IPM BLDC motor. Also, the torque ripples under various torque load conditions were reduced effectively, and this made us to expect to decrease the noise and vibration using this IPM BLDC motor. In addition, the target motor specification could be achieved at decreased manufacturing cost than the conventional IPM BLDC motor.

Also, the usage of thick PMs in the proposed asymmetrical half-type IPM BLDC motor makes it possible to use the PMs which have the high residual magnetic flux density, high grade PM, without demagnetization. Because of this reason, downsizing the motor is more advantageous than that of the conventional IPM BLDC motor.

In conclusion, it is possible to obtain high performance by the proposed asymmetrical half-type IPM BLDC motor under the same requirements of motor characteristics without increasing motor size, and this makes us to expect the proposed asymmetrical half-type IPM BLDC motor to be implemented in many fields.

References

[1] K. J. Kang, G. H. Jang, and S. J. Sung, "Frequency characteristics of BEMF, cogging torque and UMF in a HDD spindle motor due to unevenly magnetized PM," *IEEE Trans. on Magnetics*, Vol. 49, No. 6, pp. 2578-2581, Jun. 2013.

[2] H. S. Kim, Y. M. You, and B. I. Kwon, "Rotor shape optimization of interior permanent magnet BLDC motor according to magnetization direction," *IEEE Trans. on Magnetics*, Vol. 49, No. 5, pp. 2193-2196, May 2013.

[3] P. Upadhayay and K. R. Rajagopal, "Torque ripple reduction using magnet pole shaping in a surface mounted permanent magnet BLDC motor," in *Proc. 2013 International Conference on Renewable Energy Research and Applications (ICRERA)*, pp. 516-521, Oct. 2013.

[4] Z. Azar, Z. Q. Zhu, and G. Ombach, "Influence of electric loading and magnetic saturation on cogging torque, back-EMF and torque ripple of PM machines," *IEEE Trans. on Magnetics*, Vol. 48, No. 10, pp. 2650-2658, Oct. 2012.

[5] W. Q. Chu and Z. Q. Zhu, "Investigation of torque ripples in permanent magnet synchronous machines with skewing," *IEEE Trans. on Magnetics*, Vol. 49, No. 3, pp. 1211-1220 Mar. 2013.

[6] F. Zhao, T. A. Lipo, and B. I. Kwon, "A novel two-phase permanent magnet synchronous motor modeling for torque ripple minimization," *IEEE Trans. on Magnetics*, Vol. 49, No. 5, pp. 2355-2358, May 2013.

[7] J. Asama, M. Amada, M. Takemoto, A. Chiba, T. Fukao, and A. Rahman, "Voltage characteristics of a consequent-pole bearingless PM motor with concentrated windings," *IEEE Trans. on Magnetics*, Vol. 45, No. 6, pp. 2823-2826, Jun. 2009.

[8] T. Yamada, Y. Nakano, J. Asama, A. Chiba, T. Fukao, T. Hoshino, and A. Nakajima, "Outer rotor consequent-pole bearingless motor with improved start-up characteristics," *IEEE Trans. on Magnetics*, Vol. 44, No. 11, pp. 4273-4276, Nov. 2008.

[9] J. Asama, D. Kanehara, T. Oiwa, and A. Chiba, "Development of a compact centrifugal pump with a two-axis actively positioned consequent-pole bearingless motor," *IEEE Trans. on Industry Applications*, Vol. 50, No. 1, pp. 288-295, Jan./Feb. 2014.

[10] Y. S. Sim, N. Niguchi, and K. Hirata, "A novel half-type permanent magnet structure of IPM BLDC motor," in *Proc. 2015 IEEE Magnetics Conference (INTERMAG)*, FY-05, May. 2015.

Yosub Sim

received the B.E. degree from Kyungpook National University in 2009 and M.E. degree from Andong National University in 2011. He was a researcher at the Hyundai Maritime Research Institute of Hyundai Heavy Industries Co., Ltd. from 2011 to 2013. He is currently a ph. D. course student at the Department of Adaptive Machine Systems, Graduate School of Engineering in Osaka University.

Noboru Niguchi

received the B.S., M.S., and D.E. degrees from Osaka University, Japan, in 1998, 2000, and 2011, respectively. He is currently an assistant professor at the Department of Adaptive Machine Systems, Graduate School of Engineering in Osaka University.

Katsuhiro Hirata

received the B.E. degree from Osaka University in 1982 and D.E. degree from Doshisha University in 1996, respectively. He was a researcher at the R&D lab., Matsushita Electric Work Ltd. from 1982 to 2005. He joined Osaka University in 2005. He is presently a professor at the Department of Adaptive Machine Systems, Graduate School of Engineering in Osaka University.